



**HAL**  
open science

## **GABA(B) receptor activation triggers BDNF release and promotes the maturation of GABAergic synapses.**

Hervé Fiorentino, Nicola Kuczewski, Diabe Diabira, Nadine Ferrand, Menelas N. Pangalos, Christophe Porcher, Jean-Luc Gaiarsa

### ► To cite this version:

Hervé Fiorentino, Nicola Kuczewski, Diabe Diabira, Nadine Ferrand, Menelas N. Pangalos, et al.. GABA(B) receptor activation triggers BDNF release and promotes the maturation of GABAergic synapses.. *Journal of Neuroscience*, 2009, 29 (37), pp.11650-61. 10.1523/JNEUROSCI.3587-09.2009 . inserm-00483213

**HAL Id: inserm-00483213**

**<https://inserm.hal.science/inserm-00483213>**

Submitted on 12 May 2010

**HAL** is a multi-disciplinary open access archive for the deposit and dissemination of scientific research documents, whether they are published or not. The documents may come from teaching and research institutions in France or abroad, or from public or private research centers.

L'archive ouverte pluridisciplinaire **HAL**, est destinée au dépôt et à la diffusion de documents scientifiques de niveau recherche, publiés ou non, émanant des établissements d'enseignement et de recherche français ou étrangers, des laboratoires publics ou privés.

# GABA<sub>B</sub> Receptor Activation Triggers BDNF Release and Promotes the Maturation of GABAergic Synapses

Hervé Fiorentino,<sup>1</sup> Nicola Kuczewski,<sup>1</sup> Diabe Diabira,<sup>1</sup> Nadine Ferrand,<sup>1</sup> Menelas N. Pangalos,<sup>2</sup> Christophe Porcher,<sup>1</sup> and Jean-Luc Gaiarsa<sup>1</sup>

<sup>1</sup>Institut de Neurobiologie de la Méditerranée, Inserm (Institut National de la Santé et de la Recherche Médicale), Unité 901, and Université de La Méditerranée, 13273 Marseille Cedex 09, France, and <sup>2</sup>Wyeth Research, Discovery Research Neurosciences, Monmouth Junction, New Jersey 08852

GABA, the main inhibitory neurotransmitter in the adult brain, has recently emerged as an important signal in network development. Most of the trophic functions of GABA have been attributed to depolarization of the embryonic and neonatal neurons via the activation of ionotropic GABA<sub>A</sub> receptors. Here we demonstrate a novel mechanism by which endogenous GABA selectively regulates the development of GABAergic synapses in the developing brain. Using whole-cell patch-clamp recordings on newborn mouse hippocampi lacking functional GABA<sub>B</sub> receptors (GABA<sub>B</sub>-Rs) and time-lapse fluorescence imaging on cultured hippocampal neurons expressing GFP-tagged brain-derived neurotrophic factor (BDNF), we found that activation of metabotropic GABA<sub>B</sub> receptors (GABA<sub>B</sub>-Rs) triggers secretion of BDNF and promotes the development of perisomatic GABAergic synapses in the newborn mouse hippocampus. Because activation of GABA<sub>B</sub>-Rs occurs during the characteristic ongoing physiological network-driven synaptic activity present in the developing hippocampus, our results reveal a new mechanism by which synaptic activity can modulate the development of local GABAergic synaptic connections in the developing brain.

## Introduction

The proper development of highly organized structures in the CNS is a complex process that determines appropriate connectivity in the adult. Neurotransmitters released during spontaneous and experience-driven synaptic activity play a crucial role in the formation of neuronal networks (Katz and Shatz, 1996; Zhang and Poo, 2001). The most well documented example is glutamate, the major excitatory transmitter in the vertebrate CNS, which regulates nearly all aspects of neuronal network formation from migration to synaptogenesis (Zhang and Poo, 2001; Manent and Represa, 2007). Recent advances have shown that GABA acts beyond its classical inhibitory role and also functions as an important developmental signal by regulating proliferation, migration, growth, and synapse formation (Ben-Ari et al., 2007). With the observation that the activation of chloride-permeable GABA<sub>A</sub> receptors (GABA<sub>A</sub>-Rs) depolarizes developing neurons (Cherubini et al., 1991), it was proposed that part of the trophic action of GABA relies on membrane depolarization and subsequent activation of voltage-dependent calcium channels (Ben-Ari et al., 2007). Consistent with this hypothesis, early conversion of GABA-induced depolarization into hyperpolarization impaired synapse formation and dendritic development of the target neurons both *in vitro* (Chudotvorova et al., 2005) and *in vivo*

(Ge et al., 2006; Cancedda et al., 2007; Wang and Kriegstein, 2008; Reynolds et al., 2008).

In addition to ionotropic GABA<sub>A</sub>-Rs, GABA also binds to metabotropic GABA<sub>B</sub>-Rs. These receptors are ubiquitously expressed at early stages of development, even before synapses are formed (Fritschy et al., 1999; Behar et al., 2001; López-Bendito et al., 2002, 2004), and are activated by endogenous GABA released during early network-driven synaptic activity (McLean et al., 1996; Obrietan and Van den Pol, 1999; Catsicas and Mobbs, 2001; López-Bendito et al., 2003). Although GABA<sub>B</sub>-R activity has been reported to modulate cortical neuronal migration (Behar et al., 1996, 2001; López-Bendito et al., 2003), little attention has been paid to the possible contribution of GABA<sub>B</sub>-Rs in the functional development of neuronal networks.

In the present study, we tested the ability of CA3 hippocampal pyramidal cells to develop functional synaptic connections in the absence of functional GABA<sub>B</sub>-Rs. We found that activation of GABA<sub>B</sub>-Rs selectively promotes the development of hippocampal GABAergic synapses via the induction of brain-derived neurotrophic factor (BDNF) secretion. We further show that this process occurs during physiological patterns of synaptic activity. This study reveals a novel role of GABA<sub>B</sub>-Rs in regulating the self-refinement of GABAergic synaptic connections in the developing brain.

## Materials and Methods

All animal experiments were carried out according to the guidelines laid down by the Inserm animal welfare committee and the European Communities Council Directive of 24 November 1986 (86/609/EEC).

**Intact hippocampal formation and slice preparation.** Experiments were performed on intact hippocampal formation (IHF) and hippocampal slices obtained from newborn [postnatal day 1 (P1) to P24] GABA<sub>B1</sub> receptor subunit knock-out (GABA<sub>B1</sub>-KO) and wild-type (GABA<sub>B1</sub>-WT) mice (Prosser et al., 2001) and BDNF-KO and BDNF-WT mice

Received July 24, 2009; accepted Aug. 8, 2009.

This work was supported by Inserm, Centre National de la Recherche Scientifique, and Agence Nationale pour la Recherche (ANR). H.F. was a recipient of a Ministère de la Recherche et de l'Éducation fellowship. N.K. was a recipient of Fondation pour la Recherche Médicale and ANR fellowships. We wish to thank Drs. I. Medina, R. Khazipov, and M. Phillips for critical reading of this manuscript, Dr. V. Lessmann for the generous gift of BDNF-GFP cDNA, and S. Corby and C. Pellegrino for technical help.

Correspondence should be addressed to Jean-Luc Gaiarsa, Institut de Neurobiologie de la Méditerranée, Parc scientifique de Luminy, BP 13, 13273 Marseille Cedex 09, France. E-mail: gaiarsa@inmed.univ-mrs.fr.

DOI:10.1523/JNEUROSCI.3587-09.2009

Copyright © 2009 Society for Neuroscience 0270-6474/09/2911650-12\$15.00/0

(The Jackson Laboratory). The procedure for the preparation of the intact IHFs was similar to that previously described (Khalilov et al., 1997). Brains were removed from anesthetized (350 mg/kg chloral hydrate, i.p.) animals and immersed into ice-cold (2–4°C) artificial CSF (ACSF) of the following composition (in mM): 126 NaCl, 3.5 KCl, 2 CaCl<sub>2</sub>, 1.3 MgCl<sub>2</sub>, 1.2 NaH<sub>2</sub>PO<sub>4</sub>, 25 NaHCO<sub>3</sub>, and 11 glucose, pH 7.4, when equilibrated with 95% O<sub>2</sub> and 5% CO<sub>2</sub>. The hippocampi were then incubated for 12–16 h at 32°C in ACSF (oxygenated with 95% O<sub>2</sub> and 5% CO<sub>2</sub>) alone or supplemented with different drugs. After the incubation, hippocampal slices (600 μm thick) were cut with a McIlwain tissue chopper and kept in ACSF at 25°C for 60 min before use. Slices were then transferred to a submerged recording chamber and perfused with ACSF (3 ml/min) at 34°C. For each experiment, half of the dissected hippocampi were incubated in control conditions, and the other half incubated in treated conditions. Electrophysiological recordings on slices obtained from control and treated hippocampi were performed on the same day.

**Electrophysiological recordings.** Whole-cell patch-clamp recordings of CA3 pyramidal neurons were performed with an Axopatch 200B amplifier (Molecular Devices). To record miniature activity, borosilicate microelectrodes (4–8 MΩ) were filled with the following solution (in mM): 110 CsCl, 30 potassium gluconate, 10 HEPES, 1.1 EGTA, 0.1 CaCl<sub>2</sub>, 4 MgATP, 0.3 NaGTP, 5-(and-6)-tetramethylrhodamine biocytin (rhodamine, 0.5–1%), pH = 7.25, osmolarity = 275 mosmol/L. Criteria for accepting a recording included a resting potential of <–55 mV, an R<sub>i</sub> of >400 MΩ, and an R<sub>s</sub> of <25 MΩ. Capacitance, input, and series resistances were measured online with Acquis Software (Biologic).

Miniature GABA<sub>A</sub> receptor-mediated postsynaptic currents (mGABA<sub>A</sub>-PSCs) were isolated in the presence of the ionotropic glutamatergic receptor antagonists [10 μM 2,3-dihydroxy-6-nitro-7-sulfonyl-benzo [f]quinoxaline (NBQX), 40 μM D-2-amino-5-phosphoaleric acid (D-APV)] and tetrodotoxin (1 μM TTX) and recorded at a holding potential of –70 mV. Miniature glutamatergic postsynaptic currents were recorded in the presence of TTX (1 μM) and the GABA<sub>A</sub> receptor antagonist bicuculline (10 μM). Neurons were clamped at –70 mV. The currents were stored on an Axoscope 8.1 (Molecular Devices) and analyzed off-line with the Mini Analysis program (Synaptosoft 5.1). The fact that no false events would be identified was confirmed by visual inspection for each experiment. To generate the average PSCs, multiple overlapping events were discarded, and the remaining events were aligned on their rising phase. In the figures, the histograms were constructed using miniature PSCs recorded for 10–30 min. To determine the probability of presence of giant depolarizing potentials (GDPs), an average of 13 ± 6 cells (ranging from *n* = 3 at P24 to *n* = 23 at P1) were recorded in GABA<sub>B1</sub>-WT slices and 14 ± 7 cells (ranging from *n* = 3 at P24 to *n* = 27 at P2) in GABA<sub>B1</sub>-KO slices.

Peak-scaled analysis of mGABA<sub>A</sub>-PSCs was performed as described by Traynelis et al. (1993) using Mini Analysis program (Synaptosoft 5.1). For each recording, we verified the absence of correlation between the decay time course and peak amplitude of mGABA<sub>A</sub>-PSCs. For each recording, we used between 50 and 200 events and eliminated all events with a decay time distorted by multiple peaks or anomalous noise. Each individual event was scaled to the peak of the mean waveform of the averaged event and subtracted. The mean variance was plotted against mean current. The plot was well fit by a parabolic function that yields the single-channel current *i*<sub>0</sub> and the number of channels contributing to mGABA<sub>A</sub>-PSCs, *N*<sub>0</sub>. From *i*<sub>0</sub>, the single-channel conductance *γ* can be calculated.

Paired-pulse relationship (PPR) of GABAergic synapses impinging onto CA3 pyramidal neurons was measured using pairs of identical stimuli at a 100 ms interval, delivered at a frequency of 0.01 Hz with a bipolar tungsten electrode placed in the CA3 stratum radiatum. The resulting pairs of postsynaptic GABA<sub>A</sub> currents (GABA<sub>A</sub>-PSCs) were isolated in the presence of 10 μM CNQX, 40 μM D-APV, and 5 μM CGP55845. PPR was measured as the following amplitude ratio: second GABA<sub>A</sub>-PSCs/first GABA<sub>A</sub>-PSCs. Average PPR values were calculated from 20–30 paired stimulations.

**Neuron reconstruction and morphometric analysis.** Biocytin filling was done using the whole-cell patch-clamp technique. Briefly, after whole-

cell access, biocytin (1% in internal pipette solution) filling was done for 15 min. The slices were then fixed in PFA–PBS at 4°C overnight, and the biocytin-filled neurons were visualized using the avidin–biotin method. For 3-D reconstruction, a dendritic tree was digitized directly from the sections by use of a 20× objective on a Nikon microscope, equipped with a motorized stage and coupled to a computer running NeuroLucida software (MicroBrightfield), thereby allowing for *x–z* coordinates of digitized points to be stored and analyzed.

**Immunohistochemistry.** Brains from P7 mice were fixed in 4% paraformaldehyde (overnight). Cryostat-cut hippocampal sections (30 μm) were preincubated (1 h) in PBS–Triton X-100 (0.3%)–goat serum (3%) and then coincubated overnight at 4°C with antibodies to glutamic acid decarboxylase (Chemicon MAB351) and synaptophysin (Chemicon AB9272). Slices were washed with PBS, and Alexa Fluor 488 donkey antibody to mouse IgG (FluoProbes) and Cy3 donkey antibody to rabbit IgG (Chemicon) were applied (2 h). Sections were visualized with confocal microscopy (LSM 510, Zeiss). Five areas were sampled per animal, in the stratum radiatum and the stratum pyramidale. After the recording sessions, the optical sections were displayed in the form of digital images of 1024 × 1024 pixels and processed using the ImageJ software (NIH, Bethesda, MD; <http://rsb.info.nih.gov/ij/>). All the pictures were reviewed to set a threshold to optimize the representation of puncta, and then the same threshold was applied to all images. The GAD65-labeled area fraction, defined as the percentage of GAD65-immunopositive pixels per field (1024 × 1024 pixels), and the size of GAD65 puncta were measured. The proportion of colocalized immunoreactivity (IR) was expressed as the ratio: synaptophysin and GAD65 colocalized area/synaptophysin IR area or GAD65 IR area. For each section, counts were performed blindly in slices taken from three WT and three KO animals.

**Cell cultures and transfections.** Neurons from postnatal day 0 rat hippocampus were dissociated using trypsin and plated on coverslips coated with polyethylenimine as previously described (Kuczewski et al., 2008b). Eleven days after plating, neurons were transfected with cDNAs coding for BDNF-GFP (gift from Dr. V. Lessmann, Institute of Physiology, Otto-von-Guericke University Magdeburg, Magdeburg, Germany) according to the OZ Biosciences protocol (Buerli et al., 2007). After transfection, the cultures were incubated at 30°C in 5% CO<sub>2</sub>. Immunostaining confirmed that BDNF-GFP is targeted to the dendrite and packed into secretory granules of the regulated pathway of secretion (Kuczewski et al., 2008b).

**Time-lapse imaging.** Real-time imaging was performed as previously described (Kuczewski et al., 2008b). Fluorescence intensity was measured from dendritic regions containing clusters of BDNF-GFP with ImageJ software after subtraction of background fluorescence. Clusters in which the fluorescence intensity varied during the 5 min control period by >5% were discarded from the analysis. Fluorescence decreases caused by photobleaching and constitutive release were corrected by subtracting the extrapolation of the fluorescence decrease in the first 5 min over the whole recording time. Values are plotted as the percentage of the fluorescence intensity of the last frame before stimulation. Percentage variation in the text and statistical analysis were calculated by comparing the relative fluorescence of the interval –100 to 0 s (control) with that of 400–500 s (after stimuli).

**Surface GFP immunofluorescence staining.** The procedure for surface BDNF-GFP immunostaining was similar to that previously described (Kuczewski et al., 2008b). Briefly, after being washed in ACSF, the living cultures were incubated at 4°C for 1 h in the presence of an anti-GFP antibody (10 μg/ml; Molecular Probes). Cultures were then washed with 0.1 M PBS (4°C, pH 7.4) and fixed for 15 min with 4% paraformaldehyde–4% sucrose. After fixation, the neurons were exposed to a saturating concentration (10 μg/ml) of either anti-rabbit secondary antibody coupled to Cy3 (FluoProbes) for 1.5 h under a nonpermeabilized condition. Quantifications were performed with ImageJ. Surface-bound BDNF-GFP on BDNF-GFP-expressing neurons was expressed as the following ratio: Cy3 and BDNF-GFP colocalized area/BDNF-GFP area.

**Phospho-CREB activation and immunocytochemistry.** The procedure for phospho-CREB activation and immunocytochemistry was similar to that previously described (Kuczewski et al., 2008b). Briefly, 1 d before stimulation (at 13 DIV) one-half of the culture medium was changed to

MEM with 2% B27 supplement. To reduce the basal level of CREB phosphorylation, cultures were incubated for 30 min in TTX (1  $\mu$ M). Five minutes before stimulation, NBQX (10  $\mu$ M), D-APV (40  $\mu$ M), and bicuculline (20  $\mu$ M) were added to medium. The cultures were then stimulated with baclofen (50  $\mu$ M) for 10 min in the absence or presence of TrkB-IgG (2  $\mu$ g/ml) or CGP55845 (10  $\mu$ M). Five to 10 min after stimulation, neurons were fixed for 15 min (4% paraformaldehyde) at 4°C and rinsed several times. Coverslips were then preincubated in PBS–Triton-100 (0.1%)–goat serum (3%) for 1 h at room temperature and incubated overnight with mouse anti-CREB (1:1000) and rabbit anti-phospho-CREB (pCREB, 1:1000) antibodies (Cell Signaling Technology). Immunoreactivities for pCREB and CREB were detected with an Alexa 488-coupled (A488) rabbit secondary antibody (1:500; Fluor-Probes) and a Cy3-coupled mouse secondary antibody (1:500; Jackson ImmunoResearch Laboratories), respectively. All procedures were performed in phosphate-free solution containing 140 mM NaCl, 5 mM KCl, and 10 mM HEPES-Na, pH 7.4. Images were acquired with an LSM 510 laser scanning confocal microscope (Zeiss). The acquisition of A488 (pCREB) and then Cy3 (CREB) was sequential to avoid overlap of excitation and emission of fluorescence. The optical sections were digitized (1024  $\times$  1024 pixels) and processed using ImageJ software. The pCREB-to-CREB intensity ratio was expressed as means value ratio of the pCREB-A488 staining intensity versus the CREB-Cy3 staining intensity.

**ELISA.** Brains of wild-type, GABA<sub>B1</sub>-KO, and BDNF heterozygote mice were rapidly removed from their skulls at P6. Hippocampi were rapidly dissected out, weighed, and snap frozen in liquid nitrogen and stored at –80°C. BDNF was extracted from hippocampi by mechanical homogenization in a buffer containing 100 mM Tris–HCl, pH 7.0, containing 1 M NaCl, 4 mM EDTA, 2% Triton X-100, and the protease inhibitors 10  $\mu$ g/ml aprotinin, 10  $\mu$ g/ml leupeptin, and 17  $\mu$ g/ml PMSF. Homogenates were centrifuged at 14,000  $\times$  g for 20 min. Supernatants were collected and analyzed with a commercial two-antibody sandwich ELISA (BDNF E<sub>max</sub> immunoassay system; Promega) according to the protocol of the manufacturer. The total protein content of each supernatant was measured with a Bradford protein assay. The BDNF level was expressed as the ratio of BDNF to the total soluble protein concentration. There was no significant difference in the weight of GABA<sub>B1</sub>-WT and GABA<sub>B1</sub>-KO hippocampi (9.87  $\pm$  0.31 mg/hippocampi vs 9.12  $\pm$  0.56 mg/hippocampi, respectively).

**Drugs.** NBQX, D-APV, bicuculline, and CGP55845 were purchased from Tocris Cookson. Tetrodotoxin and baclofen were purchased from Sigma. k252a was from Calbiochem. TrkB-IgG and TrkC-IgG were from R&D Systems.

## Results

### Miniature GABAergic synaptic activity is altered in mice lacking functional GABA<sub>B</sub> receptors

To address the contribution of GABA<sub>B</sub>-Rs to the development of the hippocampal circuit, we recorded miniature GABA<sub>A</sub> and glutamatergic-receptor-mediated postsynaptic currents (mGABA<sub>A</sub>-PSCs and mGlu-PSCs, respectively) from hippocampal CA3 pyramidal cells from P6 to P8 GABA<sub>B1</sub>-KO mice, which display a complete loss of GABA<sub>B</sub> receptor function (Prosser et al., 2001). The frequency of mGABA<sub>A</sub>-PSCs was significantly reduced in GABA<sub>B1</sub>-KO (0.73  $\pm$  0.12 Hz in GABA<sub>B1</sub>-KO,  $n$  = 13) when compared with their wild-type littermates (1.61  $\pm$  0.26 Hz,  $n$  = 10,  $p$  = 0.03) (Fig. 1A,B). This decrease in frequency was observed at all developmental stages studied (i.e., from P1 to P10) (Fig. 1C; supplemental Fig. 1, available at www.jneurosci.org as supplemental material). The mean amplitude, coefficient of variation of amplitude (CV<sub>a</sub>), and kinetic properties of mGABA<sub>A</sub>-PSCs were unchanged (Fig. 1B; supplemental Fig. 1, available at www.jneurosci.org as supplemental material). In contrast to mGABA<sub>A</sub>-PSCs, the average frequency of mGlu-PSCs was not different between GABA<sub>B1</sub>-WT (0.11  $\pm$  0.017 Hz,  $n$  = 10) and GABA<sub>B1</sub>-KO (0.11  $\pm$  0.016 Hz,  $n$  = 12) P6–P8

neurons. The other parameters of mGlu-PSCs were also unchanged (supplemental Fig. 2, available at www.jneurosci.org as supplemental material). The membrane capacitance of the recorded cells, an indicator of neuronal size (Colin-Le Brun et al., 2004) (supplemental Fig. 3, available at www.jneurosci.org as supplemental material), was not different between GABA<sub>B1</sub>-WT and GABA<sub>B1</sub>-KO (Fig. 1B; supplemental Fig. 1, available at www.jneurosci.org as supplemental material), suggesting that the morphological development of the target CA3 pyramidal cells was not affected. This observation was confirmed by quantitative morphometric analysis of intracellularly biocytin-loaded CA3 pyramidal neurons (Fig. 1D–G). Therefore, the development of GABAergic synapses is selectively impaired in mice lacking functional GABA<sub>B</sub>-Rs.

### Blockade of GABA<sub>B</sub>-Rs *in vitro* mimics the deficit in GABAergic transmission observed in GABA<sub>B1</sub>-KO mice

In a previous study, we showed that the factors required for the functional maturation of GABAergic synapses *in vivo* are preserved in the IHFs *in vitro* (Colin-Le Brun et al., 2004). We therefore used this preparation to overcome the potential pitfalls of genetic manipulations often observed in KO animals. IHFs obtained from P1 GABA<sub>B1</sub>-WT mice were incubated at 32°C for 12–16 h in oxygenated control ACSF or with the GABA<sub>B</sub>-R antagonist CGP55845 (5  $\mu$ M). After the incubation period, hippocampal slices were prepared to record mGABA<sub>A</sub>-PSCs. In slices obtained from CGP55845-treated IHFs, the frequency of mGABA<sub>A</sub>-PSCs was significantly lower compared with control IHFs [0.107  $\pm$  0.024 Hz ( $n$  = 11) vs 0.247  $\pm$  0.049 Hz ( $n$  = 10),  $p$  = 0.031] (Fig. 1H). The other mGABA<sub>A</sub>-PSC parameters were unchanged (supplemental Fig. 4a, available at www.jneurosci.org as supplemental material). P1 IHFs obtained from GABA<sub>B1</sub>-KO mice were also incubated in control ACSF. The mean frequency of mGABA<sub>A</sub>-PSCs (0.117  $\pm$  0.026 Hz,  $n$  = 8) was significantly lower compared with control GABA<sub>B1</sub>-WT IHFs ( $p$  = 0.046) but similar to the value obtained in CGP55845-treated GABA<sub>B1</sub>-WT IHFs (Fig. 1H). The other mGABA<sub>A</sub>-PSC parameters were unchanged (supplemental Fig. 4a, available at www.jneurosci.org as supplemental material). Therefore, the pharmacological blockade of the GABA<sub>B</sub>-Rs *in vitro* reproduces the deficit in GABAergic transmission observed in GABA<sub>B1</sub>-KO mice, showing that it reflects the absence of GABA<sub>B</sub>-R activation by endogenous GABA.

### Reduced perisomatic GABAergic synapses in mice lacking GABA<sub>B</sub> receptors

We next asked whether the deficit in GABAergic synaptic transmission resides in the presynaptic or the postsynaptic site. We first performed a peak-scaled variance analysis of mGABA<sub>A</sub>-PSCs which allows an estimate of the mean unitary conductance and the number of channels open at the peak of the synaptic current (Traynelis et al., 1993) and found no difference between GABA<sub>B1</sub>-KO ( $n$  = 6) and GABA<sub>B1</sub>-WT ( $n$  = 11) neurons (Fig. 2A–C). To detect possible changes in the probability of GABA release, we then measured the paired-pulse ratio and CV<sub>a</sub> of evoked GABA<sub>A</sub>-PSCs. We found no difference between GABA<sub>B1</sub>-WT and GABA<sub>B1</sub>-KO mice ( $n$  = 5 for both) (Fig. 2D–F). Finally, to investigate possible changes in the density of GABAergic terminals, we performed immunolabeling against GAD65, the synthetic enzyme for GABA. Double immunostaining against GAD65 and synaptophysin confirmed that GAD65 staining corresponds to GABAergic terminals (supplemental Fig. 5a–c, available at www.jneurosci.org as supplemental material). Quantitative analysis shows that, compared with the GABA<sub>B1</sub>-WT

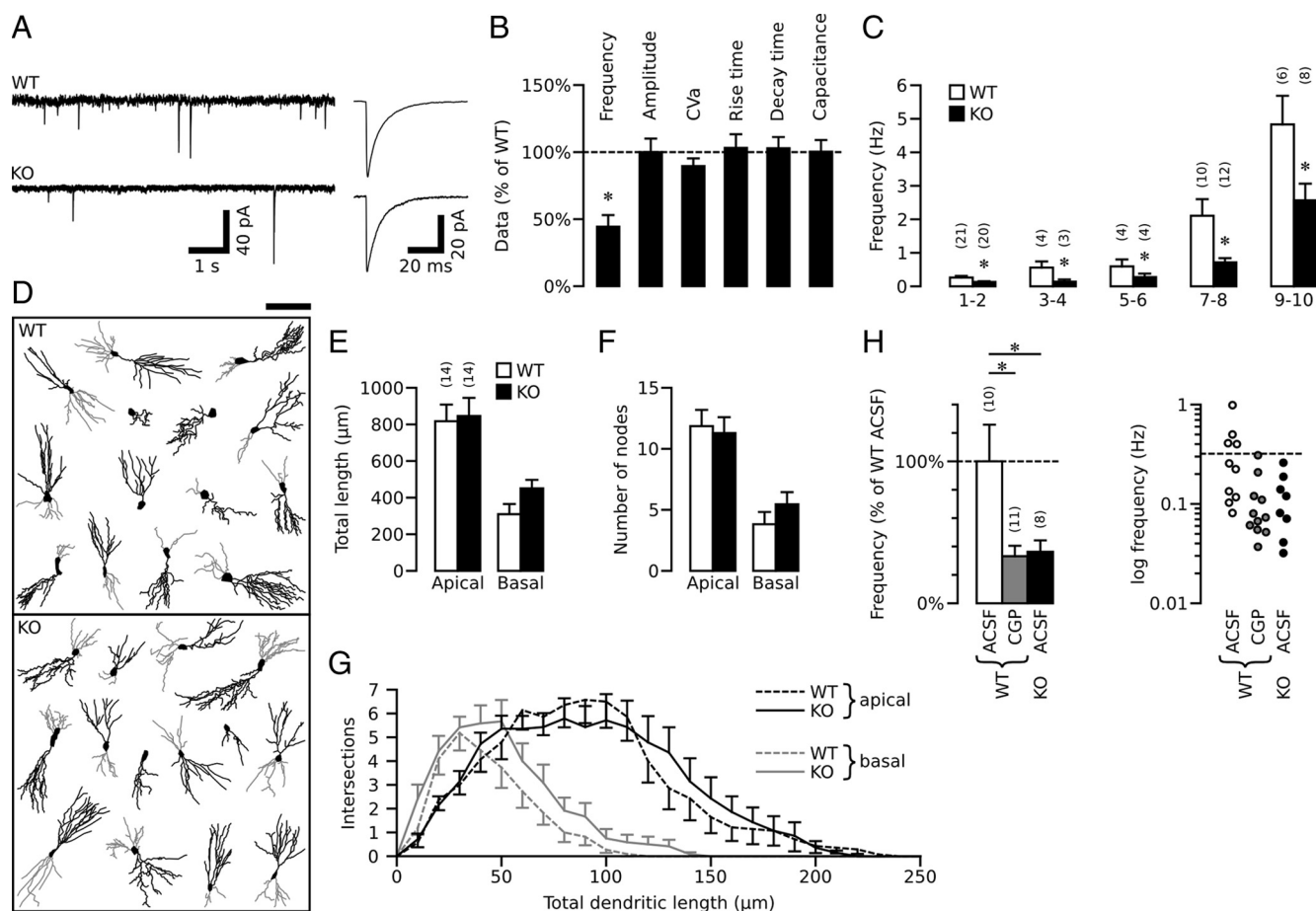


**Figure 1.** Miniature GABAergic activity is impaired in GABA<sub>B1</sub>-KO hippocampal slice. **A**, Representative traces of mGABA<sub>A</sub>-PSCs. Averaged mGABA<sub>A</sub>-PSCs ( $n = 30$ ) are shown at an expanded time scale. **B**, Summary plot of the mGABA<sub>A</sub>-PSC parameters and cell capacitance in GABA<sub>B1</sub>-KO mice at P6–P8 expressed as percentage of GABA<sub>B1</sub>-WT values. **C**, Summary plot of the mGABA<sub>A</sub>-PSC frequency in recordings from GABA<sub>B1</sub>-WT (open bars) and GABA<sub>B1</sub>-KO (filled bars) mice at different postnatal developmental stages. **D**, Two-dimensional projection of three-dimensional reconstruction of biocytin-filled P6–P7 CA3 pyramidal cells. Scale bar, 100 μm. **E, F**, Summary plot of the total apical and basal dendritic length (**E**) and dendritic branching point (**F**) of the biocytin-filled CA3 pyramidal cells of GABA<sub>B1</sub>-KO and GABA<sub>B1</sub>-WT mice. The average membrane capacitance was  $35.9 \pm 3.8$  pF for the GABA<sub>B1</sub>-WT pyramidal cells and  $38.2 \pm 3.1$  pF for the GABA<sub>B1</sub>-KO pyramidal cells.  $n = 14$  for each genotype. **G**, Sholl analysis of biocytin-filled CA3 pyramidal neurons obtained from GABA<sub>B1</sub>-KO and GABA<sub>B1</sub>-WT mice. The number of intersections within each concentric ring (10 μm beginning from the soma) is plotted versus the distance from the soma.  $n = 14$  for each genotype. **H**, Left, Summary plot of the mGABA<sub>A</sub>-PSC frequency in recordings from GABA<sub>B1</sub>-WT intact hippocampi incubated *in vitro* for 12–16 h in control condition (ACSF) or with CGP55845 (CGP; 5 μM), and from GABA<sub>B1</sub>-KO intact hippocampi incubated *in vitro* for 12–16 h in control condition (ACSF). Right, Logarithmic plot of the mGABA<sub>A</sub>-PSC frequency in recordings from GABA<sub>B1</sub>-WT and GABA<sub>B1</sub>-KO intact hippocampi incubated in the corresponding conditions. Each symbol represents the result of one single cell. The dashed line represents the mean value obtained from GABA<sub>B1</sub>-WT incubated in ACSF. In this and following figures,  $*p < 0.05$ , and the number of cells recorded is shown within brackets.

hippocampi, the labeled area fraction was reduced by ~20% in the stratum pyramidale of GABA<sub>B1</sub>-KO ( $p = 0.001$ ), while the average size of GAD-positive puncta was unchanged ( $n = 5$  pairs of mice, 5 sections per mouse) (Fig. 2*G–I*). There was, however, no difference in the labeled area fraction and average size of GAD65-positive puncta in the stratum radiatum of GABA<sub>B1</sub>-KO and GABA<sub>B1</sub>-WT hippocampi (Fig. 2*G–I*). Similar results were obtained with synaptophysin, a presynaptic marker (supplemental Fig. 5*d,e*, available at [www.jneurosci.org](http://www.jneurosci.org) as supplemental material). Although functional presynaptic modifications cannot be completely excluded, together these data suggest that the deficit in GABAergic synaptic activity observed in GABA<sub>B1</sub>-KO mice results at least in part from a decrease in the density of proximal GABAergic terminals.

**GABA<sub>B</sub>-Rs are primarily activated by spontaneous network-driven synaptic activity**

We next asked whether and when GABA<sub>B</sub>-Rs are activated during ongoing synaptic activity. To address this point, we investigated the

effect of the GABA<sub>B</sub>-R antagonist CGP55845 on GABA<sub>B1</sub>-WT slices. We found that the duration of GDPs, the characteristic primitive network-driven pattern of synaptic activity (Ben-Ari et al., 1989), was significantly increased in the presence of CGP55845 (5 μM) (from  $0.757 \pm 0.146$  s to  $1.738 \pm 0.617$  s,  $n = 8$ ,  $p = 0.0002$ ) (Fig. 3*A*). However, when applied in the presence of NBQX (10 μM) and D-APV (40 μM), to isolate spontaneous GABA<sub>A</sub>-PSCs, CGP55845 had no significant effect on the frequency, amplitude and charge transfer of sGABA<sub>A</sub>-PSCs in GABA<sub>B1</sub>-WT neurons ( $n = 9$ ) (Fig. 3*B,C*). In agreement with previous findings that GABA<sub>B</sub>-Rs are activated by concomitant release of GABA from several interneurons (Scanziani, 2000), these data show that the activation of GABA<sub>B</sub>-Rs by endogenous GABA required the presence of spontaneous GDPs.

**The lack of GABA<sub>B</sub>-R activation is responsible for the deficit in GABAergic transmission**

Network construction is modulated by the level and pattern of spontaneous synaptic activity generated in the developing ner-

vous system. Thus, the deficit in GABAergic synaptic transmission observed in the GABA<sub>B1</sub>-KO could be accounted for by alterations in spontaneous synaptic activity resulting from the lack of functional GABA<sub>B</sub>-Rs. We therefore characterized the spontaneous synaptic activity generated in the GABA<sub>B1</sub>-KO. We found that GDPs were present in both GABA<sub>B1</sub>-WT and GABA<sub>B1</sub>-KO hippocampal slices from P1 to P10 and progressively disappeared by the end of the second postnatal week (Fig. 4*A, B*). No difference in timing of the disappearance of GDPs was observed between the two groups (Fig. 4*B*). There was also no difference in the frequency or amplitude of GDPs between GABA<sub>B1</sub>-KO ( $n = 33$ ) and GABA<sub>B1</sub>-WT ( $n = 40$ ) mice (Fig. 4*C, D*). However, GDP duration was two- to threefold longer in GABA<sub>B1</sub>-KO slices ( $1630 \pm 381$  ms,  $n = 40$ ) compared with WT ( $740 \pm 97$  ms,  $n = 33$ ,  $p = 0.02$ ) (Fig. 4*A, E*). The longer GDPs in GABA<sub>B1</sub>-KO slices are network-driven synaptic events because they were recorded with field electrodes and abolished by TTX ( $1 \mu\text{M}$ ) (data not shown). As expected, application of CGP55845 ( $5 \mu\text{M}$ ) had no effect on GDP duration in GABA<sub>B1</sub>-KO slices ( $1555 \pm 72$  ms in CGP55845,  $n = 4$ ). These data therefore show that GDPs are longer in GABA<sub>B1</sub>-KO mice and that the lengthening of GDPs results from the lack of functional GABA<sub>B</sub>-R-mediated inhibition.

We next asked whether the deficit in GABAergic transmission observed in hippocampi deficient in GABA<sub>B</sub>-Rs is due to the lack of GABA<sub>B</sub>-R activity per se or is an indirect consequence of the lack of GABA<sub>B</sub>-R activity, i.e., the lengthening of GDP duration. To address this point, P1 WT IHFs were incubated for 12–16 h in the presence of TTX ( $1 \mu\text{M}$ ) to block action potential-dependent activity and GDPs. Since GABA<sub>B</sub> receptors are activated during GDPs, we hypothesized that blockade of GDPs with TTX treatment would reduce activation of GABA<sub>B</sub>-R and lead to a GABAergic deficit similar to that observed in GABA<sub>B</sub>-R-deficient hippocampi. We found that mGABA<sub>A</sub>-PSC frequency was indeed significantly reduced in TTX-treated IHFs ( $0.158 \pm 0.037$  Hz,  $n = 15$ ) compared with control IHFs ( $0.270 \pm 0.036$  Hz,  $n = 15$ ,  $p = 0.045$ ) (Fig. 4*F*). The other mGABA<sub>A</sub>-PSC parameters were unchanged (supplemental Fig. 4*b*, available at [www.jneurosci.org](http://www.jneurosci.org) as supplemental material). We next attempted to rescue the deficit induced by TTX with the specific GABA<sub>B</sub>-R agonist baclofen. Baclofen ( $5 \mu\text{M}$  for 12–16 h) completely rescued the TTX-induced deficit [from  $0.158 \pm 0.037$  Hz ( $n = 15$ ) to  $0.383 \pm 0.076$  Hz ( $n = 11$ ), respectively,  $p = 0.023$ ] (Fig. 4*F*; supplemental Fig. 4*b*, available at [www.jneurosci.org](http://www.jneurosci.org) as supplemental material). Finally, we investigated

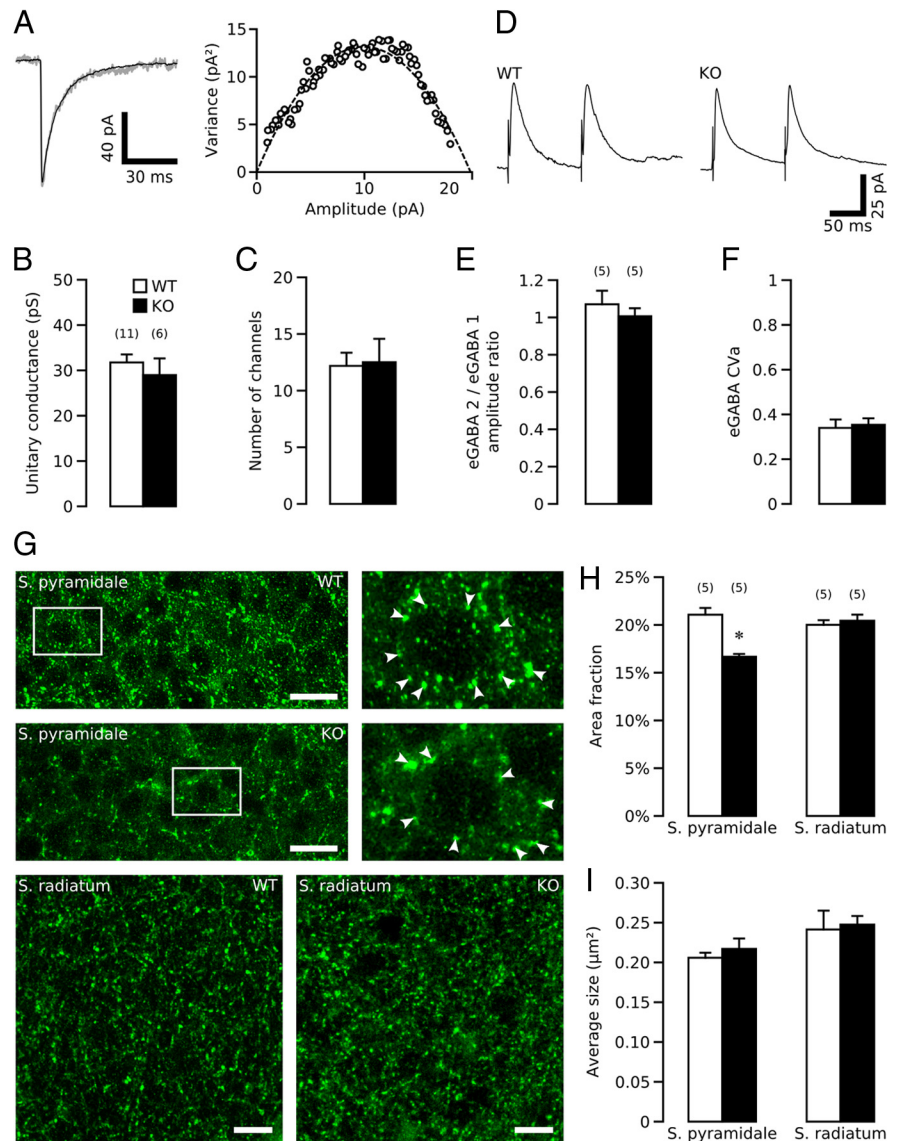


**Figure 2.** Presynaptic reduction in the number of perisomatic GABAergic terminals in GABA<sub>B1</sub>-KO hippocampi. **A**, Example of mGABA<sub>A</sub>-PSCs superimposed to the scaled mean waveform and associated relationship between mean mGABA<sub>A</sub>-PSCs amplitude and variance recorded from a representative GABA<sub>B1</sub>-KO neuron. **B, C**, Summary plot of the unitary conductance (**B**) and the number of GABA<sub>A</sub> channels at the peak of the mGABA<sub>A</sub>-PSCs (**C**) in GABA<sub>B1</sub>-WT (open bars) and GABA<sub>B1</sub>-KO (filled bars) mice. **D**, Representative averaged ( $n = 20$ ) evoked GABA<sub>A</sub>-PSCs from GABA<sub>B1</sub>-WT and KO mice (interstimulus = 100 ms). **E, F**, Summary plot of the paired-pulse ratio (**E**) and the coefficient of variation (**F**) of evoked GABA<sub>A</sub>-PSCs in GABA<sub>B1</sub>-WT (open bars) and GABA<sub>B1</sub>-KO (filled bars) mice. Both GABA<sub>B</sub>-R-dependent and GABA<sub>B</sub>-R-independent PPRs have been reported for eGABA<sub>A</sub>-PSCs in hippocampus. The PPR experiment were therefore performed in the presence of the GABA<sub>B</sub>-R antagonist CGP55845 ( $5 \mu\text{M}$ ) in both GABA<sub>B1</sub>-KO mice and GABA<sub>B1</sub>-WT. **G**, Microscopic confocal images showing GAD65-positive puncta in the strata pyramidale and radiatum of GABA<sub>B1</sub>-WT and GABA<sub>B1</sub>-KO hippocampi at postnatal day 7. Scale bars,  $10 \mu\text{m}$ . **H, I**, Summary plot of the fraction area of GAD65 fluorescence (**H**) and average size of GAD65 fluorescent puncta (**I**) in GABA<sub>B1</sub>-WT (open bars) and GABA<sub>B1</sub>-KO (filled bars). S., Stratum.

the consequences of treatment with baclofen alone, which also blocked GDPs (Tosetti et al., 2004) while activating GABA<sub>B</sub>-Rs. We found that incubation with baclofen ( $5 \mu\text{M}$ ) had no significant effect on mGABA<sub>A</sub>-PSC frequency ( $0.390 \pm 0.082$  Hz,  $n = 11$ ) when compared with control WT IHFs (Fig. 4*F*; supplemental Fig. 4*b*, available at [www.jneurosci.org](http://www.jneurosci.org) as supplemental material). Together, these data show that the deficit in GABAergic synaptic transmission observed in GABA<sub>B</sub>-R-deficient IHFs is not a consequence of abnormal synaptic activity but rather results from the lack of GABA<sub>B</sub>-R activation during ongoing synaptic activity.

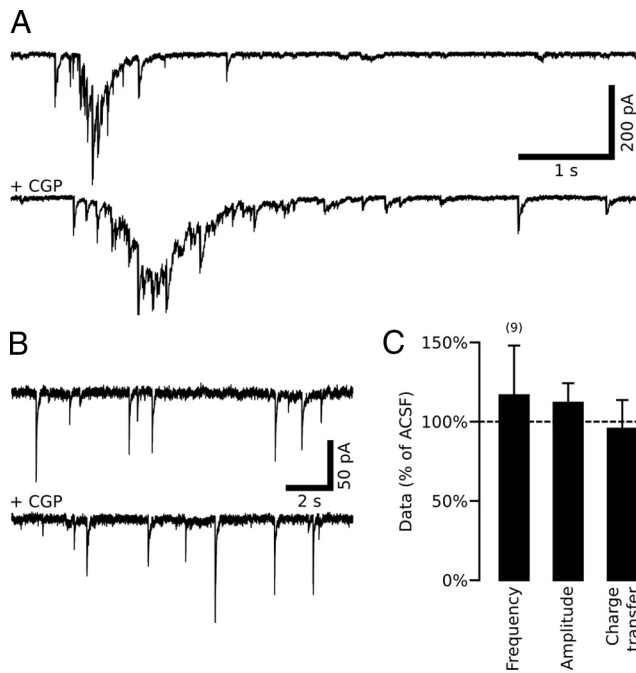


**Figure 3.** GABA<sub>B</sub>-Rs are primarily activated during spontaneous network-driven synaptic activity. **A**, Representative current traces of spontaneous GDPs recorded in GABA<sub>B1</sub>-WT pyramidal neurons in control conditions and with the GABA<sub>B</sub>-R antagonist, CGP55845 (5 μM). **B**, Representative traces of spontaneous GABA<sub>A</sub> receptor-mediated postsynaptic currents (sGABA<sub>A</sub>-PSCs) recorded in the presence of NBQX (10 μM) and D-APV (40 μM) with or without CGP55845 (5 μM). **C**, Summary plot of the effect of CGP55845 on sGABA<sub>A</sub>-PSC frequency, amplitude, and charge transfer in GABA<sub>B1</sub>-WT neurons expressed as percentages relative to control conditions (ACSF).

**GABA<sub>B</sub>-Rs and BDNF signaling interact to regulate the formation of functional GABAergic synapses**

We next asked how activity-dependent activation of GABA<sub>B</sub>-Rs translates into functional development of GABAergic synapses. Considering that BDNF is a powerful modulator of GABAergic synapse development (Lessmann et al., 2003), the recent observation that GABA<sub>B</sub>-R activity increases BDNF expression in cultured hippocampal neurons (Ghorbel et al., 2005) prompted us to test the possible contribution of BDNF-tropomyosin-related kinase (TrkB) receptor signaling to this synaptic development. P1 WT IHFs were incubated for 12–16 h with k252a (200 nM), a membrane-permeable inhibitor of protein tyrosine kinase. In k252a-treated IHFs, the frequency of mGABA<sub>A</sub>-PSCs was reduced compared with control IHFs [0.270 ± 0.036 Hz (n = 15) vs 0.105 ± 0.028 Hz (n = 14), p = 0.002] (Fig. 5A). The other mGABA<sub>A</sub>-PSC parameters were unchanged (supplemental Fig. 4c, available at www.jneurosci.org as supplemental material). The deficit induced by k252a was not rescued by baclofen [0.116 ± 0.026 Hz k252a-treated IHFs (n = 10) and 0.105 ± 0.028 Hz (n = 14) in k252a/baclofen-treated IHFs] (Fig. 5A; supplemental Fig. 4c, available at www.jneurosci.org as supplemental material). Moreover, when incubated with k252a, the GABA<sub>B</sub>-R antagonist had no further effect on mGABA<sub>A</sub>-PSCs [0.088 ± 0.024 Hz (n = 11) in CGP55845/k252a-treated IHFs vs 0.105 ± 0.028 Hz (n = 14) in k252a-treated IHFs] (Fig. 5A; supplemental Fig. 4c, available at www.jneurosci.org as supplemental material). These data show that GABA<sub>B</sub>-Rs promote the functional maturation of GABAergic synapses by means of a cascade involving tyrosine kinase signaling.

P1 WT IHFs were then incubated with the BDNF scavenger TrkB-IgG (1 μg/ml) or with the NT3 scavenger TrkC-IgG (1

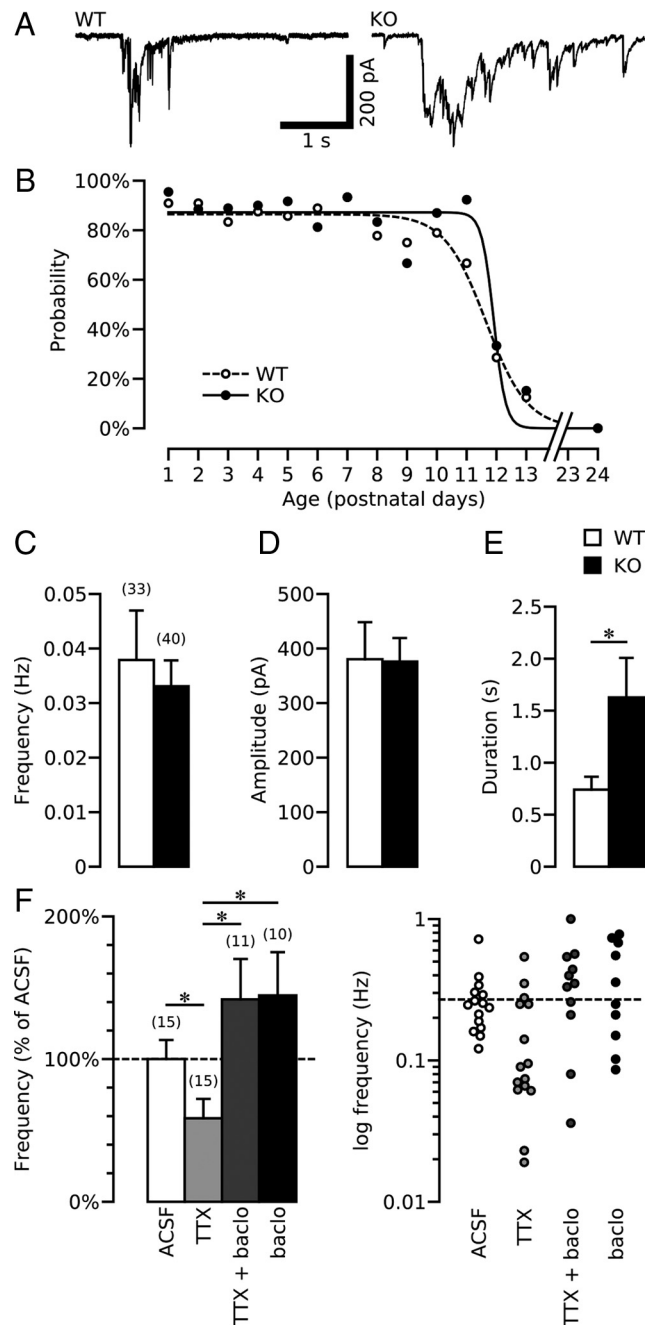
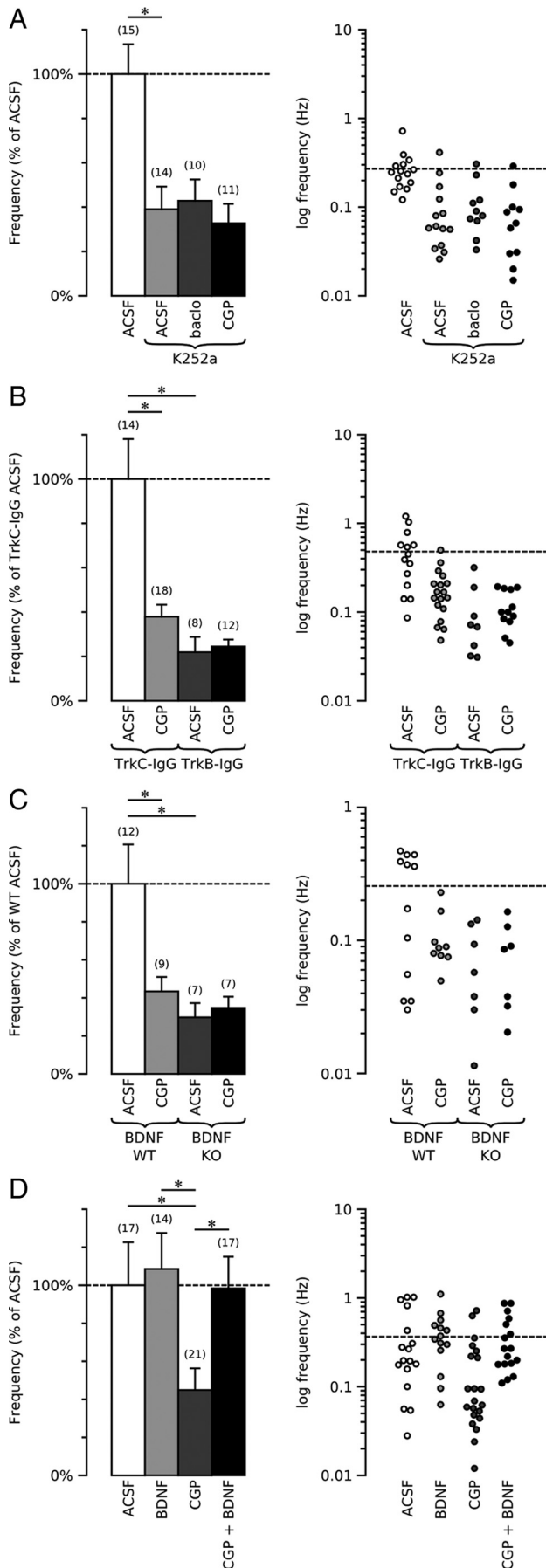


**Figure 4.** Characterization of synaptic activity in the developing mouse hippocampus. **A**, Representative current traces of spontaneous GDPs recorded in GABA<sub>B1</sub>-WT and KO CA3 pyramidal neurons. **B**, Plot of the percentage of cells showing GDPs at different postnatal stages of development in GABA<sub>B1</sub>-WT (open symbols) and GABA<sub>B1</sub>-KO (filled symbols). An average of 13 ± 6 cells (ranging from n = 3 at P24 to n = 23 at P1) were recorded in GABA<sub>B1</sub>-WT slices, and 14 ± 7 cells (ranging from n = 3 at P24 to n = 27 at P2) in GABA<sub>B1</sub>-KO slices were also recorded to construct this graph. The Boltzmann fit shows that there is no significant difference in the disappearance of GDPs between GABA<sub>B1</sub>-WT (dashed line) and GABA<sub>B1</sub>-KO (dark line). **C–E**, Summary plot of GDP frequency (**C**), amplitude (**D**), and duration (**E**) in GABA<sub>B1</sub>-WT (open bars) and GABA<sub>B1</sub>-KO (filled bars). **F**, Left, Summary plot of the mGABA<sub>A</sub>-PSC frequency in recordings from GABA<sub>B1</sub>-WT intact hippocampi incubated *in vitro* for 12–16 h in control condition (ACSF), in the presence of TTX (1 μM) alone, TTX and baclofen (5 μM), and baclofen alone. Right, Logarithmic plot of the mGABA<sub>A</sub>-PSC frequency in recordings from GABA<sub>B1</sub>-WT and GABA<sub>B1</sub>-KO intact hippocampi incubated in the corresponding conditions. Each symbol represents the result of one single cell. The dashed line represents the mean value obtained from GABA<sub>B1</sub>-WT incubated in ACSF. baclo, Baclofen.



$\mu\text{g/ml}$ ). The frequency of mGABA<sub>A</sub>-PSCs was significantly reduced in TrkB-IgG-treated IHFs ( $0.105 \pm 0.033$  Hz,  $n = 8$ ) compared with TrkC-IgG-treated IHFs ( $0.481 \pm 0.087$  Hz,  $n = 14$ ,  $p = 0.001$ ) (Fig. 5B). The other mGABA<sub>A</sub>-PSC parameters were not affected (supplemental Fig. 4d, available at www.jneurosci.org as supplemental material). The GABA<sub>B</sub>-R antagonist had no further effect on mGABA<sub>A</sub>-PSC frequency when incubated with TrkB-IgG ( $0.117 \pm 0.015$  Hz,  $n = 12$ ) (Fig. 5B; supplemental Fig. 4d, available at www.jneurosci.org as supplemental material) but significantly decreased the frequency of mGABA<sub>A</sub>-PSCs when incubated with TrkC-IgG ( $0.481 \pm 0.087$  Hz,  $n = 14$ ,  $p = 0.006$  compared TrkC-IgG-treated IHF) (Fig. 5B; supplemental Fig. 4d, available at www.jneurosci.org as supplemental material). These data show that endogenous GABA and BDNF, acting on GABA<sub>B</sub>-Rs and TrkB-Rs, respectively, interact to promote the functional maturation of hippocampal GABAergic synapses.

To confirm the requirement of GABA<sub>B</sub>-R and BDNF interaction for the functional maturation of GABAergic synapses, P1 IHFs obtained from BDNF-KO and WT littermates were incubated for 12–16 h in control ACSF or with CGP55845 ( $5 \mu\text{M}$ ). Incubation with the GABA<sub>B</sub>-R antagonist had no effect on the frequency of mGABA<sub>A</sub>-PSCs recorded from BDNF-KO IHFs [ $0.074 \pm 0.019$  Hz in control IHF ( $n = 8$ ) vs  $0.082 \pm 0.019$  Hz in CGP55845-treated IHFs ( $n = 8$ )] but significantly decreased the frequency of mGABA<sub>A</sub>-PSCs recorded from BDNF-WT IHFs [ $0.248 \pm 0.052$  Hz in control IHF ( $n = 12$ ) vs  $0.108 \pm 0.018$  Hz in CGP55845-treated IHFs ( $n = 9$ ),  $p = 0.03$ ] (Fig. 5C; supplemental Fig. 4f, available at www.jneurosci.org as supplemental material). Moreover, the frequency of mGABA<sub>A</sub>-PSCs from IHFs incubated in control ACSF was significantly reduced in BDNF-KO when compared with their wild-type littermates ( $p = 0.01$ ) (Fig. 5C), showing that BDNF is required for the functional maturation of hippocampal GABAergic synapses. Altogether, these data strengthen the conclusion that GABA<sub>B</sub>-Rs and BDNF interact to promote the maturation of GABAergic synapses in the developing mouse hippocampus.

To better determine the interplay between GABA<sub>B</sub>-Rs and BDNF-TrkB signaling, we attempted to rescue the deficit induced by CGP55845 with exogenous BDNF. P1 WT IHFs were incubated with CGP55845 ( $5 \mu\text{M}$ ) alone or with CGP55845 ( $5 \mu\text{M}$ ) and BDNF ( $50 \text{ ng/ml}$ ) for 12–16 h. BDNF rescued the deficit induced by CGP55845. The mGABA<sub>A</sub>-PSC frequency was  $0.165 \pm 0.042$  Hz in CGP55845-treated IHFs ( $n = 21$ ) and  $0.331 \pm 0.069$  Hz in CGP55845 and BDNF-treated IHFs ( $n = 17$ ,  $p = 0.014$ ) (Fig. 5D; supplemental Fig. 4e, available at www.jneurosci.org as supple-

**Figure 5.** GABA<sub>B</sub> and BDNF-TrkB signaling interact to promote the formation of functional GABAergic synapses. **A**, Left, Summary plot of the mGABA<sub>A</sub>-PSC frequency in recordings from GABA<sub>B1</sub>-WT intact hippocampi incubated *in vitro* for 12–16 h in control conditions (ACSF) or with K252a alone ( $200 \text{ nM}$ ), K252a plus CGP55845 ( $5 \mu\text{M}$ ), or K252a plus baclofen ( $5 \mu\text{M}$ ). **B**, Left, Summary plot of the mGABA<sub>A</sub>-PSC frequency in recordings from GABA<sub>B1</sub>-WT intact hippocampi incubated *in vitro* for 12–16 h in the presence of TrkC-IgG ( $1 \mu\text{g/ml}$ ) alone, TrkC-IgG plus CGP55845 (CGP,  $5 \mu\text{M}$ ), TrkB-IgG ( $1 \mu\text{g/ml}$ ) alone, or TrkB-IgG plus CGP55845 ( $5 \mu\text{M}$ ). **C**, Left, Summary plot of the mGABA<sub>A</sub>-PSC frequency in recordings from BDNF-WT and BDNF-KO intact hippocampi incubated *in vitro* for 12–16 h in control conditions (ACSF) or with CGP55845 ( $5 \mu\text{M}$ ). **D**, Left, Summary plot of the mGABA<sub>A</sub>-PSC frequency in recordings from GABA<sub>B1</sub>-WT intact hippocampi incubated *in vitro* for 12–16 h in control conditions (ACSF) or with BDNF ( $50 \text{ ng/ml}$ ), CGP55845 (CGP;  $5 \mu\text{M}$ ), or BDNF ( $50 \text{ ng/ml}$ ) plus CGP55845 ( $5 \mu\text{M}$ ). The graphs on the right in **A–D** represent the logarithmic plot of the mGABA<sub>A</sub>-PSC frequency in recordings from the intact hippocampi incubated in the corresponding conditions. Each symbol represents the result of one single cell. The dashed line represents the mean value obtained from GABA<sub>B1</sub>-WT incubated in ACSF.

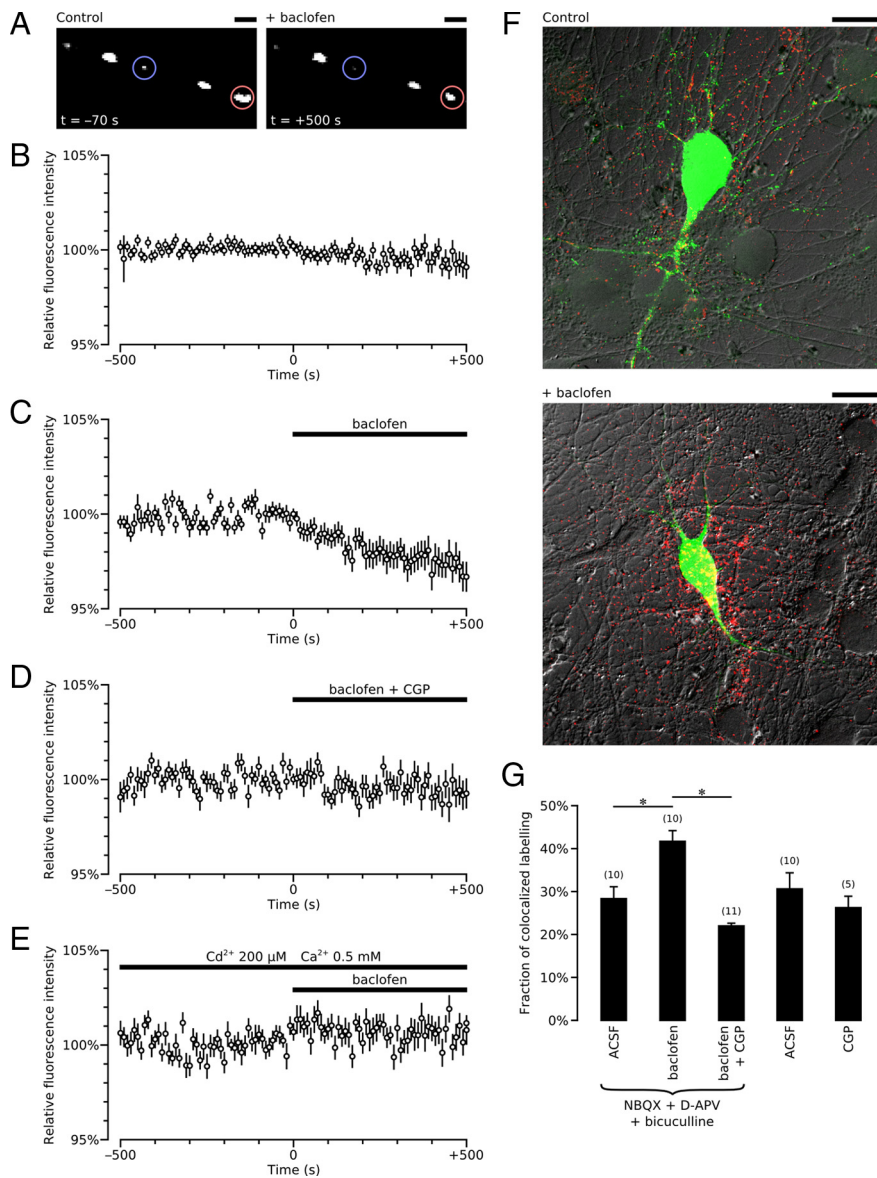


**Figure 6.** GABA<sub>B</sub>-R activation triggers BDNF-GFP secretion. **A**, Examples of dendritic BDNF-GFP granules are shown before and after baclofen application. Blue and red circles highlight examples of the BDNF-GFP clusters of fluorescence analyzed. The fluorescence was enhanced to near-saturation levels to make fluorescence variation visible. Scale bar, 5  $\mu$ m. **B–E**, Average time course of dendritic fluorescence variation in control, nonstimulated neurons (**B**) ( $n = 107$  ROIs from 23 cells), and in baclofen-stimulated neurons in the absence (**C**) ( $n = 62$  ROIs from 14 cells) or presence (**D**) ( $10 \mu$ M,  $n = 42$  ROIs from 11 cells) of CGP55845, or in nominally Ca<sup>2+</sup>-free external solution (**E**) (0.5 mM Ca<sup>2+</sup>, 200  $\mu$ M Cd<sup>2+</sup>,  $n = 31$  ROIs from 7 cells). All experiments were performed in the presence of bicuculline (20  $\mu$ M), NBQX (10  $\mu$ M), and D-APV (40  $\mu$ M). **F**, Surface staining confirmed the BDNF-GFP secretion produced by baclofen. Overlapped images showing intracellular BDNF-GFP fluorescence (green) and secreted BDNF-GFP detected using anti-GFP antibody (red) under nonpermeabilized conditions in control [bicuculline (20  $\mu$ M), NBQX (10  $\mu$ M), and D-APV (40  $\mu$ M)] and baclofen-treated sister cultures. Released BDNF-GFP that bound to the extracellular membrane of BDNF-GFP-expressing neurons appears as a yellow signal. Scale bar, 20  $\mu$ m. **G**, Quantitative analysis of surface-bound BDNF-GFP on BDNF-GFP-expressing neurons (yellow signal/green signal) in control ( $n = 10$  cells), baclofen-treated ( $n = 10$  cells), and baclofen (10  $\mu$ M) and CGP55845 (10  $\mu$ M)-treated cultures ( $n = 11$  cells) in the presence of bicuculline (20  $\mu$ M), NBQX (10  $\mu$ M), and D-APV (40  $\mu$ M). Surface-bound BDNF-GFP on BDNF-GFP-expressing neurons was also quantified in nontreated ( $n = 10$  cells) and CGP55845 (CGP; 10  $\mu$ M)-treated cultures ( $n = 5$  cells). Three different sister cultures were used in each condition.

mental material). Incubation with BDNF (50 ng/ml) alone, however, had no significant effect on mGABA<sub>A</sub>-PSC frequency when compared with control WT IHFs [0.36 ± 0.088 Hz in control IHFs ( $n = 17$ ) vs 0.407 ± 0.038 Hz in BDNF-treated IHFs ( $n = 14$ )] (Fig. 5D; supplemental Fig. 4e, available at www.jneurosci.org as supplemental material). With the observation that baclofen failed to rescue the deficit in GABAergic synaptic activity

induced by k252a (Fig. 5A), these data show that GABA<sub>B</sub>-Rs promote the maturation of GABAergic synapses by controlling the amount of available extracellular BDNF.

**Activation of GABA<sub>B</sub>-Rs triggers BDNF release**

We next asked how GABA<sub>B</sub>-Rs control extracellular BDNF availability. GABA<sub>B</sub>-Rs could modulate the production and/or secretion of BDNF. To determine whether GABA<sub>B</sub>-Rs modulate BDNF production, we measured the level of BDNF in hippocampi of GABA<sub>B1</sub>-KO and GABA<sub>B1</sub>-WT by use of an ELISA and found no significant difference (110 ± 7 pg/ml total protein vs 109 ± 10 pg/ml total protein, respectively,  $n = 5$  for both).

In an attempt to determine whether GABA<sub>B</sub>-Rs could modulate the secretion of BDNF, we sought to measure the amount of BDNF released from mouse hippocampi *in vitro* upon GABA<sub>B</sub>-R activation using ELISA. However, levels of BDNF in these samples were below the threshold for detection of the assay. We therefore examined whether activation of GABA<sub>B</sub>-Rs triggers BDNF release at the cellular level. With this aim, we transfected cultured hippocampal neurons with GFP-tagged BDNF and monitored dendritic BDNF-GFP secretion with time-lapse fluorescent imaging in living neurons. Using this approach, BDNF-GFP secretion was detectable as a decrease in intracellular GFP fluorescence intensity (Kuczewski et al., 2008b). To exclude indirect effects of synaptic activity, GABAergic and glutamatergic ionotropic receptor antagonists were present. Baclofen (10  $\mu$ M) led to a significant decrease of dendritic BDNF-GFP fluorescence intensity [−2.6 ± 0.63% change 5 min after baclofen application,  $n = 62$  regions of interest (ROIs) from 14 cells,  $p = 0.0008$  compared with control period,  $p = 0.01$  compared with nonstimulated neurons,  $n = 107$  ROIs from 23 cells] (Fig. 6A–C). The decrease in fluorescence intensity induced by baclofen was prevented by CGP55845 (10  $\mu$ M, −0.74 ± 0.53% change 5 min after baclofen application,  $n = 42$  ROIs from 11 cells,  $p = 0.03$  compared with baclofen alone) (Fig. 6D) and by nominally Ca<sup>2+</sup>-free extracellular solution (0.005 ± 0.005% change after 5 min of baclofen application,  $n = 31$  ROIs from 7 cells,  $p = 0.0006$  compared with baclofen alone) (Fig. 6E). The baclofen-induced secretion of BDNF-GFP was confirmed by surface-bound BDNF-GFP immunostaining (Kuczewski et al., 2008b). Bath-applied baclofen (10  $\mu$ M, 10 min) increases GFP staining surrounding the BDNF-GFP-expressing cell (Fig. 6F). Quantification of surface-bound

BDNF-GFP on transfected neurons shows that baclofen significantly increased BDNF-GFP release ( $n = 10$  cells for both, 3 cultures,  $p = 0.04$  compared with control) (Fig. 6G). This effect was prevented by CGP55845 ( $10 \mu\text{M}$ ,  $n = 11$  cells, 3 cultures) (Fig. 6G), which when applied alone had no effect on surface-bound BDNF-GFP in control conditions ( $n = 5$  cells, 3 cultures) (Fig. 6G).

These data show that GABA<sub>B</sub>-R activation can trigger secretion of BDNF-GFP from hippocampal neurons in culture. However, protein overexpression could have modified the release properties of BDNF. To determine whether GABA<sub>B</sub>-R activation can trigger secretion of endogenous BDNF, we used the phosphorylated form of the cAMP response element-binding protein CREB (pCREB) as a sensor of endogenous BDNF release (Kuczewski et al., 2008b). Once released, BDNF interacts with TrkB receptors to activate downstream signaling pathways. One of the most common is the ERK (extracellular signal-regulated kinase) pathway, which leads to the phosphorylation of CREB (Ghosh et al., 1994). We therefore tested whether baclofen can induce a BDNF-dependent phosphorylation of CREB. Hippocampal neuronal cultures were stimulated with baclofen (3 and  $50 \mu\text{M}$ ) for 10 min in the presence of NBQX ( $10 \mu\text{M}$ ), D-APV ( $50 \mu\text{M}$ ), and bicuculline ( $20 \mu\text{M}$ ). To rule out a possible effect of baclofen treatment on CREB synthesis and to normalize the results obtained from different cultures, the pCREB/CREB ratio was quantified (Fig. 7A, B). At  $3 \mu\text{M}$ , baclofen induced a significant increase of the pCREB/CREB ratio [ $30 \pm 11\%$  in control ( $n = 74$  cells, 3 cultures) versus  $43 \pm 7\%$  in baclofen-treated ( $n = 64$  cells, 3 cultures) cultures,  $p = 0.001$ ]. At  $50 \mu\text{M}$ , baclofen induced a threefold increase of the pCREB/CREB ratio [from  $27 \pm 5\%$  in control ( $n = 42$  cells, 3 cultures) versus  $77 \pm 13\%$  in baclofen-treated ( $n = 54$  cells, 3 cultures) cultures,  $p = 0.00008$ ] (Fig. 7B). This increase was prevented by CGP55845 ( $10 \mu\text{M}$ ,  $n = 43$  cells; 3 cultures,  $p = 0.0003$  compared with baclofen) (Fig. 7B), showing that GABA<sub>B</sub>-R activation is required. No difference in the pCREB/CREB ratio was observed when the cultures were stimulated by baclofen in the presence of the BDNF scavenger TrkB-IgG ( $2 \mu\text{g/ml}$ ,  $n = 21$  cells, 3 cultures,  $p = 0.0002$  compared with baclofen) (Fig. 7B). As expected, BDNF ( $20 \text{ ng/ml}$ ) triggered a phosphorylation of CREB and an increase in the pCREB/CREB ratio ( $n = 40$  cells, 3 cultures,  $p = 0.0001$  compared with control) (Fig. 7B). Thus, GABA<sub>B</sub>-R activation triggers secretion of endogenous BDNF.

## Discussion

GABA, the main inhibitory transmitter in the adult vertebrate brain, has recently emerged as an important signal for neuronal development. Besides its classical role in regulating synaptic activity, GABA modulates nearly all key steps of network construction from neuronal migration to experience-dependent refinement of local connections (Ben-Ari et al., 2007). Most of these effects have been attributed to the depolarizing action of GABA, which leads to a postsynaptic rise in intracellular  $\text{Ca}^{2+}$  concentration in developing neurons via the activation of chloride-permeable GABA<sub>A</sub>-Rs (Ben-Ari et al., 2007). Here, we reveal a novel mechanism by which endogenous GABA selectively regulates the development of GABAergic synapses. We found that activation of metabotropic GABA<sub>B</sub>-Rs triggers secretion of BDNF and promotes the development of GABAergic synapses in the hippocampus of newborn mice. Moreover, we show that this process occurs during ongoing physiological patterns of activity.

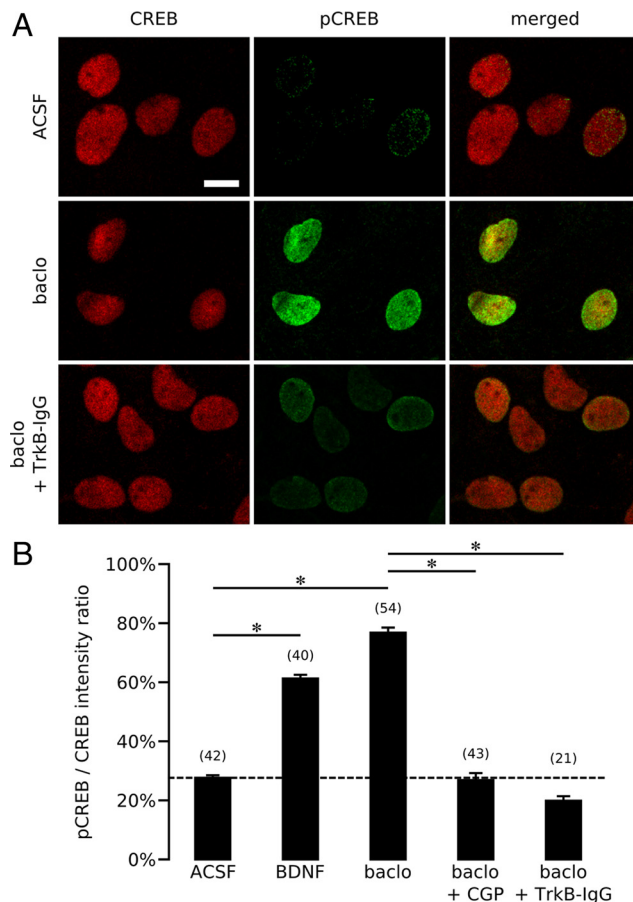


**Figure 7.** GABA<sub>B</sub>-R activation induces a BDNF-dependent phosphorylation of CREB in hippocampal neuronal cultures. **A**, Immunofluorescence signal of CREB (red, left panels) and phosphorylated CREB (pCREB, green, middle panels) in hippocampal neuronal cultures in control conditions (top panels) or treated with baclofen in the absence (middle panels) or presence (bottom panels) of TrkB-IgG. Merged images are shown on the right. Scale bar,  $10 \mu\text{m}$ . **B**, Average pCREB/CREB ratio in the different conditions. For each condition, three different sister cultures were used, and quantification was based on 7–18 cells per culture. baclo, Baclofen; CGP, CGP55845.

Our study shows that GABA<sub>B</sub>-R signaling plays a role in self-regulating inhibitory synapse development. We have identified a selective deficit in miniature GABAergic synaptic activity in GABA<sub>B1</sub>-KO hippocampal pyramidal cells that can be reproduced *in vitro* in wild-type hippocampi in which GABA<sub>B</sub>-Rs were pharmacologically blocked. Miniature GABAergic activity was also reduced in wild-type hippocampi incubated with TTX, to block action potential-dependent synaptic activity and subsequent activation of GABA<sub>B</sub>-Rs. The TTX-induced deficit was rescued by the selective GABA<sub>B</sub> receptor agonist, baclofen, showing that GABA<sub>B</sub>-R activation is required for the functional maturation of GABAergic synapses. Although we cannot completely rule out functional presynaptic modifications, we provide morphological data suggesting that the reduced GABAergic activity in GABA<sub>B1</sub>-KO mice is at least in part due to a decrease in the number of perisomatic GABAergic terminals. This result is consistent with previous findings that synaptic activity (Chattopadhyaya et al., 2004) and endogenous GABA levels (Chattopadhyaya et al., 2007) regulate cortical basket cell axon branching and perisomatic synapse formation through the activation of GABA<sub>A</sub> and GABA<sub>B</sub> receptors. Since miniature activity has been proposed to originate from proximal

GABAergic synapses (Soltesz et al., 1995), a decrease in the density of those synapses will significantly affect the frequency of mGABA<sub>A</sub>-PSCs in GABA<sub>B1</sub>-KO pyramidal cells.

The timing of disappearance of GDPs, whose generation critically depends on depolarizing action of GABA (Ben-Ari et al., 2007), was not affected between GABA<sub>B1</sub>-KO and WT mice. This result suggests that the depolarizing-to-hyperpolarizing developmental shift in GABA<sub>A</sub> receptor-mediated responses is not affected in GABA<sub>B1</sub>-KO mice. Accordingly, we found that bath-applied isoguvacine, a selective GABA<sub>A</sub>-R agonist, increased the spiking activity of CA3 pyramidal neurons during the first postnatal week of life in both GABA<sub>B1</sub>-KO and WT mice (unpublished observations). Several studies have shown that the depolarizing and excitatory action of GABA<sub>A</sub> receptors is an important signal for neuronal network development (Barbin et al., 1993; Manent et al., 2005; Cancedda et al., 2007; Wang and Kriegstein, 2008); this might explain the lack of structural alterations or modifications in the morphology of CA3 pyramidal neurons in GABA<sub>B1</sub>-KO mice.

We show that the mechanism by which GABA<sub>B</sub>-Rs promote the formation of GABAergic synapses *in vivo* likely involves BDNF secretion and subsequent activation of the TrkB signaling pathway. k252a or TrkB-IgG mimicked and occluded the deleterious effect of GABA<sub>B</sub>-R blockade, the GABA<sub>B</sub>-R antagonist had no effect on BDNF-KO mice, and GABA<sub>B</sub>-R activation triggered dendritic Ca<sup>2+</sup>-dependent secretion of BDNF in hippocampal cultures. The fact that BDNF is necessary for the maturation of GABAergic synapses has been clearly established, but the source and mechanism of its activity-dependent release have remained unexplored. So far, at least three distinct signals regulating dendritic BDNF secretion have been directly identified in neuronal cultures (Kuczewski et al., 2009): (1) tetanic stimulation of presynaptic glutamatergic fibers (Hartmann et al., 2001), (2) action potentials that propagate backwards into the dendrites (Kuczewski et al., 2008b), and (3) prolonged depolarization of the postsynaptic neuron (Magby et al., 2006). Our study provides a novel and unexpected mechanism by which synaptic activity can trigger a Ca<sup>2+</sup>-dependent dendritic release of BDNF.

Important questions remain about the cell type and the location of GABA<sub>B</sub>-Rs involved *in vivo*. Because GABAergic interneurons and glial cells do not produce neurotrophins themselves (Ernfors et al., 1990), BDNF is likely provided by CA3 pyramidal neurons (Brigadski et al., 2005) or the mossy fibers arising from dentate gyrus granular cells (Danzer and McNamara, 2004). GABA<sub>B</sub>-R activation can increase the intracellular Ca<sup>2+</sup> concentration in neurons (Shen and Slaughter, 1999; Hirono et al., 2001; New et al., 2006). A recent study has shown that the phosphorylation of  $\alpha$ -CaMKII, a critical step in BDNF secretion (Kolarow et al., 2007), is enhanced by GABA<sub>B</sub>-R activation in the developing rat hippocampus (Xu et al., 2008). Thus, postsynaptic Ca<sup>2+</sup> elevation and  $\alpha$ -CaMKII phosphorylation might underlie the GABA<sub>B</sub>-R-induced secretion of BDNF and development of GABAergic synapses that we found in the present study. Alternatively, GABA<sub>B</sub>-Rs can increase Ca<sup>2+</sup> concentration in glial cells (Kang et al., 1998; Meier et al., 2008) and indirectly trigger neuronal secretion of BDNF (Elmariah et al., 2005). Further experiments will be required to address this point.

Regulated activity-dependent release of BDNF is crucial for many different aspects of GABAergic and glutamatergic synapse development (Lu et al., 2005). However, because BDNF diffusion (Horch and Katz, 2002) and Ca<sup>2+</sup> rise are rather restricted

events, spatial proximity is required between the signal that triggers the secretion of BDNF and the target. Synaptic activation of ionotropic glutamatergic receptors has been previously reported to trigger a localized dendritic release of BDNF (Hartmann et al., 2001) and a potentiation of GABAergic synaptic activity in the developing rat hippocampus (Kuczewski et al., 2008a). However, glutamatergic synapses are restricted to the dendrites. Thus, activation of somatic GABA<sub>B</sub>-Rs might trigger the local and specific secretion of BDNF needed for the development of perisomatic GABAergic synapses. Such specificity in the control of BDNF secretion might explain why perisomatic GABAergic synapses, but not glutamatergic or dendritic GABAergic synapses, are impaired in GABA<sub>B1</sub>-KO hippocampi. Thus multiple triggers of BDNF secretion might coexist in the hippocampus. Depending on the pattern of activity generated by the neuronal network, BDNF could exert a selective control on the development of different subpopulations of GABAergic synapses. The reason why GABA<sub>B</sub>-R-mediated trophic action is selective for perisomatic GABAergic synapses remains to be clarified. One likely possibility is that the effectors linking GABA<sub>B</sub>-R activation to BDNF secretion are exclusively localized at the perisomatic level.

GABA<sub>B</sub>-Rs are located at perisynaptic or extrasynaptic sites, and thus GABA spillover is needed to activate them. GABA spillover becomes substantial during high-frequency stimulation (Isaacson et al., 1993; Xu et al., 2008) or concomitant activation of several interneurons or when the GABA uptake is blocked (Scanziani, 2000). In the developing hippocampus, most of the ongoing synaptic activity is provided by a primitive network-driven pattern, termed GDPs, present both *in vitro* (Ben-Ari et al., 1989) and *in vivo* (Leinekugel et al., 2002). GABAergic interneurons fire synchronously during GDPs (Khazipov et al., 1997). GDPs therefore fulfil the criteria for GABA<sub>B</sub>-R activation (McLean et al., 1996). Accordingly, we found that the lack of GABA<sub>B</sub>-R function in GABA<sub>B1</sub>-KO neurons resulted in lengthening of GDPs. In contrast, when GDPs were blocked in GABA<sub>B1</sub>-WT neurons, the GABA<sub>B</sub>-R antagonist had no significant effect on spontaneous GABAergic activity. Thus, the activation of GABA<sub>B</sub>-Rs required the presence of GDPs. We therefore propose that GDPs play an instructive role in the development of the hippocampal GABAergic circuit, providing the critical amount of GABA needed to activate GABA<sub>B</sub>-Rs and trigger a subsequent secretion of BDNF. Accordingly, a deficit in GABAergic synaptic activity was observed when GDPs were blocked with TTX, but not when GDPs were blocked with the GABA<sub>B</sub>-R agonist baclofen. Thus, baclofen substitutes for GDPs to activate GABA<sub>B</sub>-Rs showing that the activation of these receptors is sufficient to support a proper development of at least perisomatic GABAergic synapses. This conclusion is strengthened by the observation that the TTX-induced deficit was rescued by baclofen. Since early spontaneous network-driven activity similar to GDPs and subsequent activation of GABA<sub>B</sub>-Rs appear to occur in virtually every developing circuit (Obrietan and Van den Pol, 1999; Catsicas and Mobbs, 2001), it is possible that this mechanism is important for synaptic maturation throughout the nervous system.

## References

- Barbin G, Pollard H, Gaïarsa JL, Ben-Ari Y (1993) Involvement of GABA<sub>A</sub> receptors in the outgrowth of cultured hippocampal neurons. *Neurosci Lett* 152:150–154.
- Behar TN, Li YX, Tran HT, Ma W, Dunlap V, Scott C, Barker JL (1996) GABA stimulates chemotaxis and chemokinesis of embryonic cortical neurons via calcium-dependent mechanisms. *J Neurosci* 16:1808–1818.
- Behar TN, Smith SV, Kennedy RT, McKenzie JM, Maric I, Barker JL (2001)

- GABA(B) receptors mediate motility signals for migrating embryonic cortical cells. *Cereb Cortex* 11:744–753.
- Ben-Ari Y, Cherubini E, Corradetti R, Gaiarsa JL (1989) Giant synaptic potentials in immature rat CA3 hippocampal neurones. *J Physiol* 416:303–325.
- Ben-Ari Y, Gaiarsa JL, Tyzio R, Khazipov R (2007) GABA: a pioneer transmitter that excites immature neurons and generates primitive oscillations. *Physiol Rev* 87:1215–1284.
- Brigadski T, Hartmann M, Lessmann V (2005) Differential vesicular targeting and time course of synaptic secretion of the mammalian neurotrophins. *J Neurosci* 25:7601–7614.
- Buerli T, Pellegrino C, Baer K, Lardi-Studler B, Chudotvorova I, Fritschy JM, Medina I, Fuhrer C (2007) Efficient transfection of DNA or shRNA vectors into neurons using magnetofection. *Nat Protoc* 2:3090–3101.
- Cancedda L, Fiumelli H, Chen K, Poo MM (2007) Excitatory GABA action is essential for morphological maturation of cortical neurons *in vivo*. *J Neurosci* 27:5224–5235.
- Catsicas M, Mobbs P (2001) GABA<sub>B</sub> receptors regulate chick retinal calcium waves. *J Neurosci* 21:897–910.
- Chattopadhyaya B, Di Cristo G, Higashiyama H, Knott GW, Kuhlman SJ, Welker E, Huang ZJ (2004) Experience and activity-dependent maturation of perisomatic GABAergic innervation in primary visual cortex during a postnatal critical period. *J Neurosci* 24:9598–9611.
- Chattopadhyaya B, Di Cristo G, Wu CZ, Knott G, Kuhlman S, Fu Y, Palmiter RD, Huang ZJ (2007) GAD67-mediated GABA synthesis and signaling regulate inhibitory synaptic innervation in the visual cortex. *Neuron* 54:889–903.
- Cherubini E, Gaiarsa JL, Ben-Ari Y (1991) GABA: an excitatory transmitter in early postnatal life. *Trends Neurosci* 14:515–519.
- Chudotvorova I, Ivanov A, Rama S, Hübner CA, Pellegrino C, Ben-Ari Y, Medina I (2005) Early expression of KCC2 in rat hippocampal cultures augments expression of functional GABA synapses. *J Physiol* 566:671–679.
- Colin-Le Brun I, Ferrand N, Caillard O, Tosetti P, Ben-Ari Y, Gaiarsa JL (2004) Spontaneous synaptic activity is required for the formation of functional GABAergic synapses in the developing rat hippocampus. *J Physiol* 559:129–139.
- Danzer SC, McNamara JO (2004) Localization of brain-derived neurotrophic factor to distinct terminals of mossy fiber axons implies regulation of both excitation and feedforward inhibition of CA3 pyramidal cells. *J Neurosci* 24:11346–11355.
- Elmariyah SB, Oh EJ, Hughes EG, Balice-Gordon RJ (2005) Astrocytes regulate inhibitory synapse formation via Trk-mediated modulation of postsynaptic GABA<sub>A</sub> receptors. *J Neurosci* 25:3638–3650.
- Erfors P, Wetmore C, Olson L, Persson H (1990) Identification of cells in rat brain and peripheral tissues expressing mRNA for members of the nerve growth factor family. *Neuron* 5:511–526.
- Fritschy JM, Meskenaite V, Weinmann O, Honer M, Benke D, Mohler H (1999) GABAB-receptor splice variants GB1a and GB1b in rat brain: developmental regulation, cellular distribution and extrasynaptic localization. *Eur J Neurosci* 11:761–768.
- Ge S, Goh EL, Sailor KA, Kitabatake Y, Ming GL, Song H (2006) GABA regulates synaptic integration of newly generated neurons in the adult brain. *Nature* 439:589–593.
- Ghorbel MT, Becker KG, Henley JM (2005) Profile of changes in gene expression in cultured hippocampal neurons evoked by the GABAB receptor agonist baclofen. *Physiol Genomics* 22:93–98.
- Ghosh A, Carnahan J, Greenberg ME (1994) Requirement for BDNF in activity-dependent survival of cortical neurons. *Science* 263:1618–1623.
- Hartmann M, Heumann R, Lessmann V (2001) Synaptic secretion of BDNF after high-frequency stimulation of glutamatergic synapses. *EMBO J* 20:5887–5897.
- Hirono M, Yoshioka T, Konishi S (2001) GABA(B) receptor activation enhances mGluR-mediated responses at cerebellar excitatory synapses. *Nat Neurosci* 4:1207–1216.
- Horch HW, Katz LC (2002) BDNF release from single cells elicits local dendritic growth in nearby neurons. *Nat Neurosci* 5:1177–1184.
- Isaacson JS, Solís JM, Nicoll RA (1993) Local and diffuse synaptic actions of GABA in the hippocampus. *Neuron* 10:165–175.
- Kang J, Jiang L, Goldman SA, Nedergaard M (1998) Astrocyte-mediated potentiation of inhibitory synaptic transmission. *Nat Neurosci* 1:683–692.
- Katz LC, Shatz CJ (1996) Synaptic activity and the construction of cortical circuits. *Science* 274:1133–1138.
- Khalilov I, Esclapez M, Medina I, Aggoun D, Lamsa K, Leinekugel X, Khazipov R, Ben-Ari Y (1997) A novel *in vitro* preparation: the intact hippocampal formation. *Neuron* 19:743–749.
- Khazipov R, Leinekugel X, Khalilov I, Gaiarsa J-L, Ben-Ari Y (1997) Synchronization of GABAergic interneuronal network in CA3 subfield of neonatal rat hippocampal slices. *J Physiol* 498:763–772.
- Kolarow R, Brigadski T, Lessmann V (2007) Postsynaptic secretion of BDNF and NT-3 from hippocampal neurons depends on calcium calmodulin kinase II signaling and proceeds via delayed fusion pore opening. *J Neurosci* 27:10350–10364.
- Kuczewski N, Langlois A, Fiorentino H, Bonnet S, Marissal T, Diabira D, Ferrand N, Porcher C, Gaiarsa JL (2008a) Spontaneous glutamatergic activity induces a BDNF-dependent potentiation of GABAergic synapses in the newborn rat hippocampus. *J Physiol* 586:5119–5128.
- Kuczewski N, Porcher C, Ferrand N, Fiorentino H, Pellegrino C, Kolarow R, Lessmann V, Medina I, Gaiarsa JL (2008b) Backpropagating action potentials trigger dendritic release of BDNF during spontaneous network activity. *J Neurosci* 28:7013–7023.
- Kuczewski N, Porcher C, Lessmann V, Medina I, Gaiarsa JL (2009) Activity-dependent dendritic release of BDNF and biological consequences. *Mol Neurobiol* 39:37–49.
- Leinekugel X, Khazipov R, Cannon R, Hirase H, Ben-Ari Y, Buzsáki G (2002) Correlated burst of activity in the neonatal rat hippocampus *in vivo*. *Science* 296:2049–2052.
- Lessmann V, Gottmann K, Malsangio M (2003) Neurotrophin secretion: current facts and future prospects. *Prog Neurobiol* 69:341–374.
- López-Bendito G, Shigemoto R, Kulik A, Paulsen O, Fairén A, Luján R (2002) Expression and distribution of metabotropic GABA receptor subtypes GABABR1 and GABABR2 during rat neocortical development. *Eur J Neurosci* 15:1766–1778.
- López-Bendito G, Luján R, Shigemoto R, Ganter P, Paulsen O, Molnár Z (2003) Blockade of GABA(B) receptors alters the tangential migration of cortical neurons. *Cereb Cortex* 13:932–942.
- López-Bendito G, Shigemoto R, Kulik A, Vida I, Fairén A, Luján R (2004) Distribution of metabotropic GABA receptor subunits GABAB1a/b and GABAB2 in the rat hippocampus during prenatal and postnatal development. *Hippocampus* 14:836–848.
- Lu B, Pang PT, Woo NH (2005) The yin and yang of neurotrophin action. *Nat Rev Neurosci* 6:603–614.
- Magby JP, Bi C, Chen ZY, Lee FS, Plummer MR (2006) Single-cell characterization of retrograde signaling by brain-derived neurotrophic factor. *J Neurosci* 26:13531–13536.
- Manent JB, Represa A (2007) Neurotransmitters and brain maturation: early paracrine actions of GABA and glutamate modulate neuronal migration. *Neuroscientist* 13:268–279.
- Manent JB, Demarque M, Jorquera I, Pellegrino C, Ben-Ari Y, Aniksztejn L, Represa A (2005) A noncanonical release of GABA and glutamate modulates neuronal migration. *J Neurosci* 25:4755–4765.
- McLean HA, Caillard O, Khazipov R, Ben-Ari Y, Gaiarsa JL (1996) Spontaneous release of GABA activates GABA<sub>B</sub> receptors and controls network activity in the neonatal rat hippocampus. *J Neurophysiol* 76:1036–1046.
- Meier SD, Kafitz KW, Rose CR (2008) Developmental profile and mechanisms of GABA-induced calcium signaling in hippocampal astrocytes. *Glia* 56:1127–1137.
- New DC, An H, Ip NY, Wong YH (2006) GABAB heterodimeric receptors promote Ca<sup>2+</sup> influx via store-operated channels in rat cortical neurons and transfected Chinese hamster ovary cells. *Neuroscience* 137:1347–1358.
- Obrietan K, Van den Pol AN (1999) GABA<sub>B</sub> receptor-mediated regulation of glutamate-activated calcium transients in hypothalamic and cortical neuron development. *J Neurophysiol* 81:94–102.
- Prosser HM, Gill CH, Hirst WD, Grau E, Robbins M, Calver A, Soffin EM, Farmer CE, Lanneau C, Gray J, Schenck E, Warmerdam BS, Clapham C, Reavill C, Rogers DC, Stean T, Upton N, Humphreys K, Randall A, Geppert M, Davies CH, Pangalos MN (2001) Epileptogenesis and enhanced prepulse inhibition in GABA(B1)-deficient mice. *Mol Cell Neurosci* 17:1059–1070.
- Reynolds A, Brustein E, Liao M, Mercado A, Babilonia E, Mount DB, Drapeau

- P (2008) Neurogenic role of the depolarizing chloride gradient revealed by global overexpression of KCC2 from the onset of development. *J Neurosci* 28:1588–1597.
- Scanziani M (2000) GABA spillover activates postsynaptic GABA(B) receptors to control rhythmic hippocampal activity. *Neuron* 25:673–681.
- Shen W, Slaughter MM (1999) Metabotropic GABA receptors facilitate L-type and inhibit N-type calcium channels in single salamander retinal neurons. *J Physiol* 516:711–718.
- Soltesz I, Smetters DK, Mody I (1995) Tonic inhibition originates from synapses close to the soma. *Neuron* 14:1273–1283.
- Tosetti P, Bakels R, Colin-Le Brun I, Ferrand N, Gaiarsa JL, Caillard O (2004) Acute desensitization of presynaptic GABAB-mediated inhibition and induction of epileptiform discharges in the neonatal rat hippocampus. *Eur J Neurosci* 19:3227–3234.
- Traynelis SF, Silver RA, Cull-Candy SG (1993) Estimated conductance of glutamate receptor channels activated during EPSCs at the cerebellar mossy fiber-granule cell synapse. *Neuron* 11:279–289.
- Wang DD, Kriegstein AR (2008) GABA regulates excitatory synapse formation in the neocortex via NMDA receptor activation. *J Neurosci* 28:5547–5558.
- Xu C, Zhao MX, Poo MM, Zhang XH (2008) GABA(B) receptor activation mediates frequency-dependent plasticity of developing GABAergic synapses. *Nat Neurosci* 11:1410–1418.
- Zhang LI, Poo MM (2001) Electrical activity and development of neural circuits. *Nat Neurosci* 4 [Suppl]:1207–1214.